Journal of Materials Chemistry A

Accepted Manuscript

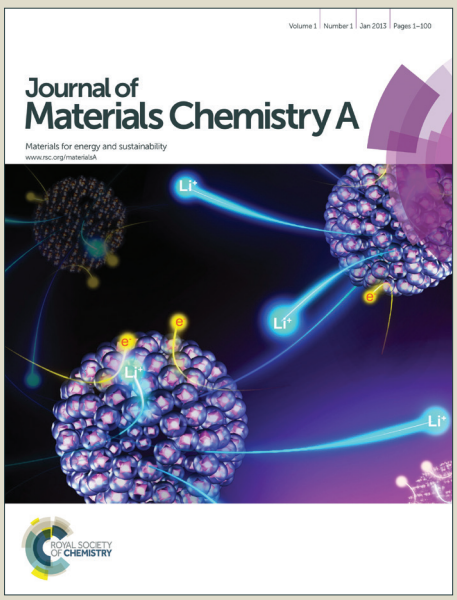

ROYAL SOCIETY OF CHEMISTRY

www.rsc.org/materialsA

Journal Name

RSCPublishing

ARTICLE

Study on a Magnetic-Cooling Material $Gd(OH)CO_3$†

Cite this: DOI: 10.1039/x0xx00000x

Yan-Cong Chen,[a] Lei Qin,[b] Zhao-Sha Meng,[a] Ding-Feng Yang,[b] Chao Wu,*[b] Zhendong Fu,[c] Yan-Zhen Zheng,*[b] Jun-Liang Liu,[a] Róbert Tarasenko,[d] Martin Orendáč,*[d] Jan Prokleška,[e] Vladimír Sechovský,[e] and Ming-Liang Tong*[a]

Received 00th January 2012,
Accepted 00th January 2012

DOI: 10.1039/x0xx00000x

www.rsc.org/

The magnetocaloric effect of a coordination polymeric material with repeating unit of $Gd(OH)CO_3$ has been experimentally studied using isothermal magnetization and heat capacity measurements. The maximum entropy change $-\Delta S_m$ reaches 66.4 J kg^{-1} K^{-1} or 355 mJ cm^{-3} K^{-1} for ΔH = 7 T and T = 1.8 K. DFT calculations show weak and competing antiferromagnetic interactions between the metal centres.

Introduction

Since Warburg discovered magnetocaloric effect (MCE) in metallic iron in 1881,[1] magnetic cooling has been proposed to be an environmentally friendly and energy-efficient cooling technique.[2] Due to the maximum MCE of a magnetic material usually occurs at the vicinity of magnetic phase transition the control of magnetic ordering is critical for certain application.[3] At room temperature, the situation is challenging as there are not many ferromagnets order nearby.[4] For low-temperatures more options are available owing to the less thermal vibration from the lattice and thus, not only ferromagnets but also paramagnets can be employed. The discovery of gadolinium gallium garnet ($Gd_3Ga_5O_{12}$, GGG) and its iron-substituted derivatives ($Gd_3(Ga_{1-x}Fe_x)_5O_{12}$, GGIG) have paved the way for magnetic cooling application from 2-20 K,[5] but there is still room for improvement (i.e. to search a better replacement and/or extend the working region).[6]

Recently, a new type of nano-scale magnetic materials have emerged in this field and been proved to be very competitive to GGG and GGIG as low-temperature refrigerants.[7-10] Such new materials have distinct advantages, such as identical size, stoichiometric composition, and providing the opportunity of rational synthesis and modification. The recipes for synthesizing such magnetic coolers have been reviewed recently,[11] from which we noticed that much effort has been focused on enhancing the ground spin state (S) according to the magnetic entropy change ($-\Delta S_m$) equation $-\Delta S_m = R\ln(2S+1)$. The ion Gd^{3+} is therefore preferred for its half-filled 4f orbital (S = 7/2) and magnetic isotropy. But Gd^{3+} has the disadvantage of large atomic weight because the gravimetric $-\Delta S_m$ is reversely proportional to the molecular weight. Moreover, as the internal 4f electrons are well covered by outer paired electrons the magnetic communications between the Gd^{3+} ions are usually weak. As such, MCE contributed from phase transition is usually minor, and better Gd(III)-based magnetic coolers (no matter measured with gravimetric or volumetric units) always commensurate with high metal/ligand ratio.

This request could be realized by using low molecular mass ligands or increasing the dimensionality - to build Gd(III)-based coordination polymers.[9-10] To achieve this goal, a ligand with multi-negative charge and high coordination number is important for counterbalancing the positive charges and meeting the high-coordination requirement of Gd^{3+} ions. To date, carboxylate ligands, especially the small acetate and formate are preferred for this purpose,[10] and the large metal/ligand ratio further leads to high mass density responsible for greater volumetric MCE.[12] In contrast to these carboxylate ligands herein we propose using carbonate instead. Because carbonate can be regarded as a condensation product of carboxylates by reducing the non-coordinating moiety, see **Scheme 1**. We expected that the high negative charge and multi-coordination sites will make CO_3^{2-} more efficient than formate and oxalate when binding Gd^{3+} ions. Moreover, the coordination topology of CO_3^{2-} based on its triangular shape is promising to induce competing magnetic interactions between metal centres, like geometrical spin-frustration, which is believed to be beneficial for enhancing MCE.[11]

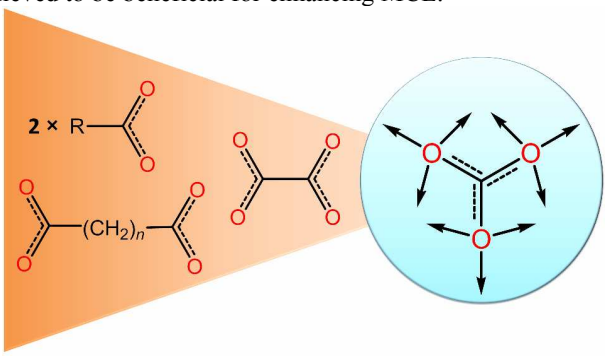

Scheme 1. A comparison of the carboxylates and carbonate. Arrows are the available coordination sites.

Driven by these two reasons, we synthesized a Gd(III) hydroxyl carbonate with repeating unit of $Gd(OH)CO_3$. This material exhibits maximum magnetic entropy change $-\Delta S_m$ up

to 67.1 J kg^{-1} K^{-1} (or 359 mJ cm^{-3} K^{-1}) and adiabatic temperature change (ΔT_{ad}) up to 24 K for ΔH = 9 T, which is comparable to the performance of GGG or GGIG.

Experimental section

Synthesis of $Gd(OH)CO_3$

METHOD A

A mixture of $GdCl_3 \cdot 6H_2O$ (0.1 mmol), malononitrile (0.2 mmol) and deioned water (5 mL) was sealed into a 23 mL Teflon-lined autoclave and heated at 180 °C for 72 h, followed by cooling to room temperature in air. Colourless crystals were washed by deionized water and dried in air (yield 50% based on Gd).

METHOD B

$GdCl_3 \cdot 6H_2O$ (2.0 mmol) and Na_2CO_3 (2.0 mmol) were mixed in H_2O (40mL) and stirred for 15 minutes at room temperature. The slurry was sealed into a 50 mL Teflon-lined autoclave and heated at 170 °C for 72 h, followed by cooling to room temperature in a rate of 3 °C h^{-1}. Colourless block crystals were isolated and washed with deionized water (yield 52.8% based on Gd).

IR data of $Gd(OH)CO_3$ (KBr cm^{-1}): 3459 (s), 2521 (w), 2340 (w), 1825 (s), 1790 (s). Anal. calcd. for $CHGdO_4$: C 5.13, H 0.43; found: C 5.31, H 0.56.

X-ray Crystallography

Powder X-ray diffraction measurements were performed on grinded polycrystalline samples at room temperature on a Bruker D8 X-Ray Diffractometer Cu Kα radiation. Single-crystal diffraction data was recorded at 150(2) K on a Rigaku R-AXIS SPIDER Image Plate diffractometer with Mo Kα radiation, solved by direct methods and refined using SHELXTL program.[13a] The metrical symmertry and space group were confirmed using PLATON program.[13b] Crystal Data and Structural Refinement are listed in **Table 1**. Further details on the crystal structure may be obtained in the ESI (**Tables S1** and **S2**) and from the Fachinformationszentrum Karlsruhe, 76344 Eggenstein-Leopoldshafen, Germany (fax: (+49)□7247-808-666; e-mail: crysdata@fiz-karlsruhe.de), by quoting the depository number CSD-426257 ($Gd(OH)CO_3$).

Physical Measurements

The magnetic measurements were performed on the polycrystalline samples using a Quantum Design MPMS XL-7 SQUID magnetometer. Low-temperature magnetic susceptibility was measured on the polycrystalline samples synthesized from method B. Low-temperature specific heat was studied on a Quantum Design PPMS with the ^{3}He option adopting standard relaxation technique.

DFT calculations

DFT calculations were performed with CASTEP code[14a]. The crystal structure of $Gd(OH)CO_3$ determined from single-crystal X-Ray Diffraction was employed for theoretical studies without further geometry optimization. Ultra-soft pseudopotentials were utilized to describe the electron-ion interactions. Exchange and correlation were described by Perdew-Burke-Ernzerh (PBE) function in the generalized gradient approximation (GGA) scheme.[14b] A kinetic energy cut-off of 600 eV was used for plane-wave expansions in the reciprocal space. The Monkhorst-Pack grid was set to 5×5×5 in the Brillouin zone of the 1×2×1-supercell.[14c] Our spin-polarized calculations predict that $Gd(OH)CO_3$ is a magnetic insulator even without adding on site repulsion U on Gd, which can be seen from the total and partial DOS plots calculated for the ferromagnetic state of $Gd(OH)CO_3$ in **Figure S4**, so we did not use the DFT plus U method.[14d]

Table 1 Crystal Data and Structural Refinement.

Chemical formula	$CHGdO_4$
Formula Mass	234.27
Crystal system	Orthorhombic
Space group	*Pnma*
Z	4
a/Å	7.0770(7)
b/Å	4.8730(9)
c/Å	8.4353(6)
Unit cell volume/Å^3	290.90(6)
Temperature/K	150(2)
ρ_{calcd} / g cm^{-3}	5.349
μ (Mo Kα) / mm^{-1}	22.608
No. of reflections measured	2591
No. of independent reflections	356
R_{int}	0.0305
R_1[a] ($I > 2\sigma(I)$)	0.0201
wR_2[b] (all data)	0.0538
Goodness of fit on F^2	1.036

[a] $R_1 = \Sigma||F_o| - |F_c||/\Sigma|F_o|$
[b] $wR_2 = [\Sigma w(F_o^2 - F_c^2)^2/\Sigma w(F_o^2)^2]^{1/2}$.

Results and discussion

Synthesis.

There are two hydrothermal ways for the synthesis of $Gd(OH)CO_3$. Method A involves the decomposition of malononitrile (NC-CH_2-CN). It is easy for cyano groups to be hydrolysed into carboxylates and amines in the hydrothermal condition (R-CN → R-$CONH_2$ →R-COO^- + NH_4^+). The former product can be further decomposed to CO_3^{2-} *via* decarboxylation and thus the $Gd(OH)CO_3$ precipitates out. The amine can act as a buffering agent to prevent the rapid hydrolysis of Gd^{3+} into $Gd(OH)_3$ or other products. Method B that involves the direct reaction of Gd^{3+} ions and carbonates is also very efficient.

Crystal Structure

The powder X-ray diffraction pattern of $Gd(OH)CO_3$ has be known for decades as it has been listed in JCPDF (#43-0604, unindexed) with an provisional formula of $Gd_2O(CO_3)_2 \cdot H_2O$. However, such an assignment cannot explain the high thermal stability of this material up to ~700 K[15a]. Without single-crystal X-ray data, the exact structure remains controversial and the crystallization into orthorhombic $P2_12_12_1$[15b] and hexagonal $P\text{-}6$[15c] space groups have also been reported. Our single-crystal diffraction data analysis reveals $Gd(OH)CO_3$ crystallizes in the orthorhombic space group *Pnma via* the hydrothermal synthesis described above, without the producing other phases, as shown in **Figure 1**.

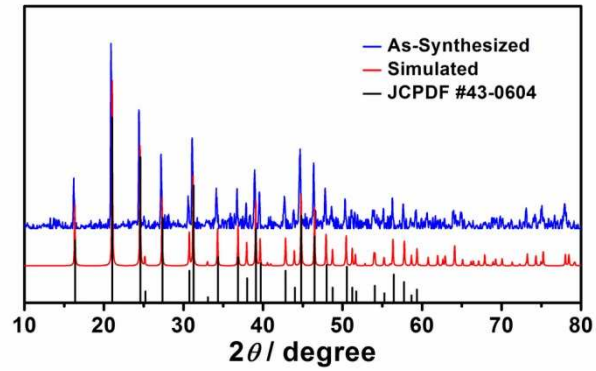

Figure 1 Powder XRD pattern of as-synthesized $Gd(OH)CO_3$ compared to the simulation from single crystal structure and the JCPDF #43-0604.

In the crystal structure, each asymmetric unit contains half of the chemical formula. The Gd^{3+} ion is 10-coordinated with six oxygen atoms from three chelating CO_3^{2-} groups, two oxygen atoms from two mono-dentate CO_3^{2-} groups, and other two oxygen atoms from two OH^- groups. The Gd···O separations are ranging from 2.29 to 2.75 Å (**Figure 2a**). The CO_3^{2-} groups are μ_5-bridging with two μ_3-O and one μ-O atoms bounding to adjacent Gd^{3+} ions (**Figure 2b**), and the hydroxyl groups are μ-bridging between Gd^{3+}, forming one-dimensional (1D) zigzag $[-Gd-(\mu\text{-}OH)-Gd-(\mu\text{-}OH)]_n$ chains along the *a* axis with the Gd···Gd separation of 3.82 Å (**Figure 3**).

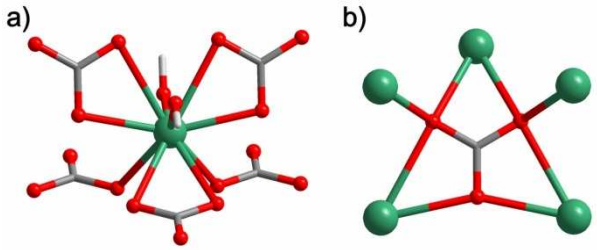

Figure 2 The coordination environment of a) Gd^{3+} and b) CO_3^{2-}. Colour Codes: Gd, green; O, red; C, grey; H, light grey.

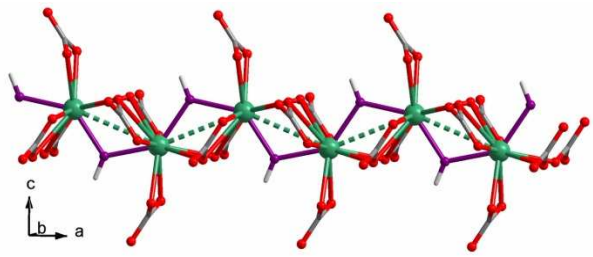

Figure 3 The 1-Dimentional Gd^{3+}-OH^- zigzag chain along the *a* axis. Colour Codes: Gd, green; O, red and purple; C, grey; H, light grey.

The network structure of $Gd(OH)CO_3$ can be depicted in two ways according to the building units. One way is to use the $[-Gd-(\mu\text{-}OH)-Gd-(\mu\text{-}OH)]_n$ chains as building units. Each of them is interlinked with six neighbours into a 3D network (**Figure 4a**). However, the six linking directions are inequivalent. Four of them are only directed by a pair of μ_3-O atoms from the μ_5-CO_3^{2-} groups in adjacent *ab*-plane. The other two directions are extended in the *ab*-plane. As shown in **Figure 4b**, the zigzag $[-Gd-(\mu\text{-}OH)-Gd-(\mu\text{-}OH)]_n$ chains are alternatively linked by opposite carbonate groups. Thus, the other way to describe the 3D structure is to use the *ab* planes as building units, which contains exactly the formula $[Gd(OH)CO_3]_n$.

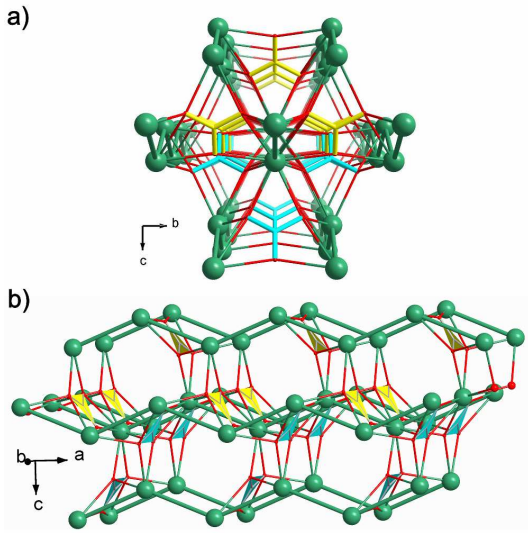

Figure 4 The inter-chain structure supported by CO_3^{2-} viewed a) along the *a* axis and b) aside from the b axis. The OH^- groups are omitted for clarity and the opposite carbonates are highlighted with yellow and blue triangles. Colour Codes: Gd, green; O, red; C, yellow, light blue and grey; H, light grey.

The dense inorganic framework structure of $Gd(OH)CO_3$ without solvent-accessible porosity also gives rise to a large density of 5.349 g cm^{-3}, which is beneficial for the volumetric MCE. Furthermore, we have found that the hydroxyl groups in the structure are μ-bridging rather than μ_3-bridging, and such a bridging mode may weaken the magnetic coupling between Gd^{3+} ions, thus is extremely favourable for a cryogenic magnetic cooler.

Magnetic Properties

Variable-temperature magnetic susceptibility measurement was performed on polycrystalline sample of $Gd(OH)CO_3$ in an applied dc field of 0.05 T (**Figure 5a**). At room temperature, the $\chi_m T$ value is 7.84 cm^3 K mol^{-1}, in good agreement with the spin-only value expected for a free Gd^{3+} ion with $g = 2$ (7.875 cm^3 K mol^{-1}). Upon cooling, $\chi_m T$ stays essentially constant until approximately 30 K, followed by gradually decreasing to the minimum of 4.68 cm^3 K mol^{-1} at 1.8 K. The inverse magnetic susceptibility ($1/\chi_m$) obeys the Curie-Weiss law with $C = 7.86$ cm^3 K mol^{-1} and $\theta = -1.05$ K, indicating weak antiferromagnetic coupling. Surprisingly, despite the large proportion of OH^- in the polymeric structure, the overall magnetic coupling characterized by the Weiss constant θ is yet weaker than in many molecular clusters and cluster-organic frameworks comprising Gd^{3+}. Such a behaviour not only arise from the difference between the μ-OH^- and μ_3-OH^- bridges, but also due to the competing magnetic interactions mediated by the CO_3^{2-} groups.

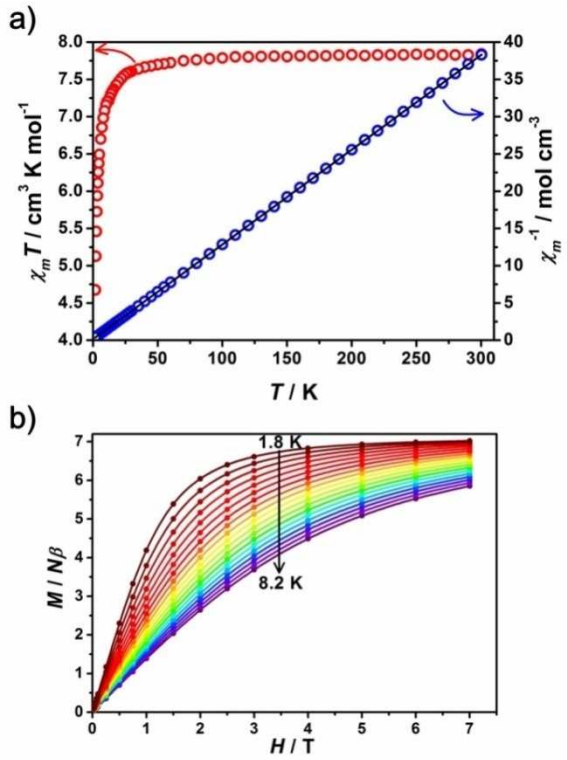

Figure 5 a) Temperature-dependencies of the magnetic susceptibility product $\chi_m T$ and inverse magnetic susceptibility $1/\chi_m$ in 1.8 K ~ 300 K with the field of 0.05 T. The black solid line represents the least-square fit for Curie-Weiss law. b) Magnetization versus field in the temperature range of 1.8 K ~ 8.2 K.

The isothermal magnetization from 1.8 K to 8.2 K were also measured (**Figure 5b**). The magnetization increases steadily with the applied field and reach the saturation value of 7.0 $N\beta$ at 1.8 K and 7 T, which is in good agreement with the expected value for a Gd^{3+} ion ($s = {}^7/_2$, $g = 2$). The large magnetization values, together with the low molecular weight and high mass density, make this material a promising candidate for cryogenic magnetic refrigeration, where the isothermal entropy change can be calculated by applying the Maxwell equation (**Figure 6**):

$$\Delta S_m(T) = \int_0^H \left[\partial M(T, H)/\partial T\right]_H dH$$

In general, the $-\Delta S_m$ values grow gradually against reducing temperature, but rise progressively with increasing applied fields, reaching a maximum of 66.4 J kg^{-1} K^{-1} (355 mJ cm^{-3} K^{-1}) at T = 1.8 K and ΔH = 7 T, close to the theoretical limiting value of 73.8 J kg^{-1} K^{-1} (395 mJ cm^{-3} K^{-1}) calculated from $R\ln(2s+1)/Mw$ with $s = {}^7/_2$ and Mw = 234.3 g mol^{-1}. The result here is already quite exciting; however the peak of $-\Delta S_m$ is still not reached in the aforementioned temperature, indicating the necessity of further investigation in the sub-Kelvin region.

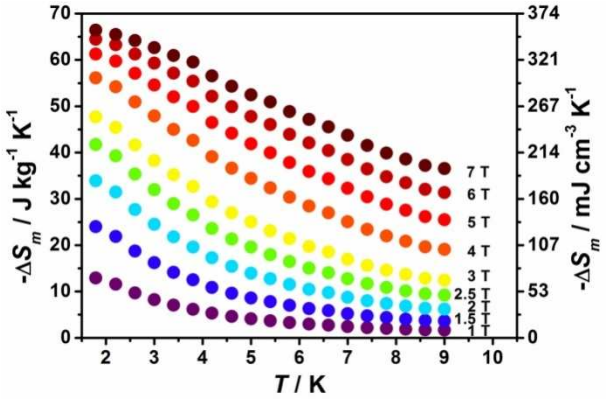

Figure 6 Temperature-dependencies of $-\Delta S_m$ for selected ΔH obtained from magnetization. The data with field variation below 1 T are omitted for clarity.

Heat Capacity

To further investigate the MCE of this material, low temperature heat capacity (C) measurements were performed in the applied fields from 0 to 9 T (**Figure 7**). Clearly, the higher temperature region is dominated by lattice contribution arising from thermal vibration, which can be well fitted to the Debye's model and yield the Debye temperature (θ_D) of 313(3) K with r_D = 7.[16] Such a high Debye temperature compared with other molecule-based materials is indicative of the rigid frameworks consisting of strong chemical bonds and light ligand atoms.[10] This is very important to yield a large ΔT_{ad} in the adiabatic demagnetization process, where the lattice vibration is forced to compensate for the variation of magnetic entropy.

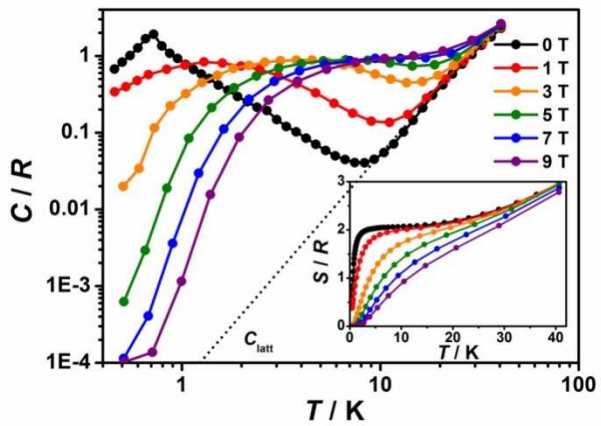

Figure 7 Temperature-dependencies of the heat capacity normalized to the gas constant in selected applied fields. The dotted line represents the lattice contribution. Inset: temperature-dependencies of the entropy obtained from heat capacity.

At lower temperatures, the heat capacity is dominated by field-dependent magnetic contribution, which shows a broad Schottky type feature caused by the splitting of the $^8S_{7/2}$ multiplet. A small sharp anomaly is observed in the zero field at approximately 0.7 K but suppressed by applied fields, indicating the emergence of a phase transition. This can be attributed to the long-range magnetic interactions mediated by the polymeric network, which is further demonstrated to be antiferromagnetic by a downturn on the χ_m-T curve (**Figure S1**). Such a behaviour is also observed in the recent reported $Gd(HCOO)_3$ around 0.8 K,[10d] however, the entropy content associated with the magnetic transition is quite low and it

makes mere impact on the cooling capability as we can see below.

From the experimental C, the entropy can be obtained by numerical integration using:

$$S(T) = \int_0^T C(T)/T dT$$

The experimental C are subsequently extrapolated, and a constant value base on the high temperature saturation value of magnetic entropy ($S_{m,\,sat} = R\ln(2s+1) = 2.08\ R$), **Figure S2**) was added to the zero-field entropy to compensate for experimental inaccessibility to absolute zero.[10a] Thus, the isothermal magnetic entropy change (ΔS_m) and the adiabatic temperature change (ΔT_{ad}) can be derived from the S-T curves (**inset of Figure 7**) by vertical and horizontal subtraction, respectively.[4]

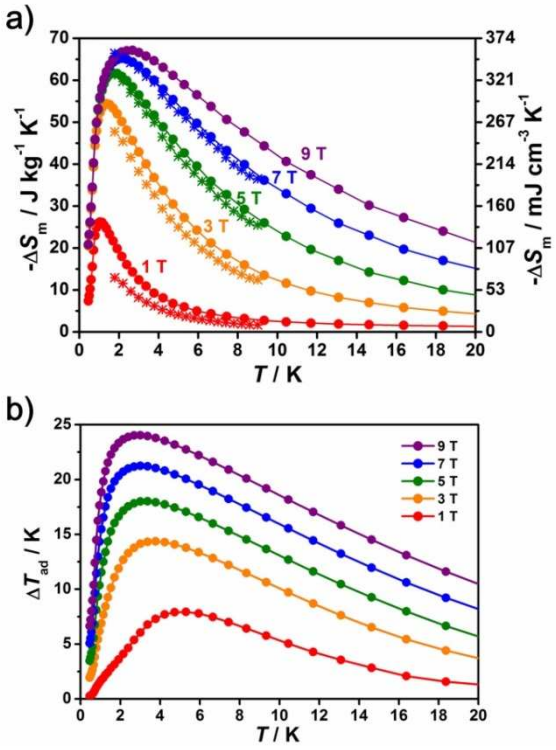

Figure 8 a) Temperature-dependencies of $-\Delta S_m$ obtained from magnetization (□) and heat capacity (●) for selected ΔH. b) Temperature-dependencies of ΔT_{ad} for selected ΔH.

The maxima of the temperature-dependent of $-\Delta S_m$ keep rising and shift to higher temperature with increasing applied fields (**Figure 8**). Indeed, the $-\Delta S_{m,\,max}$ for $\Delta H = 1$ T is already up to 26.2 J kg^{-1} K^{-1} (140 mJ cm^{-3} K^{-1}), and it increases sharply when higher fields are applied, namely 54.4 J kg^{-1} K^{-1} (291 mJ cm^{-3} K^{-1}) for $\Delta H = 3$ T and 67.1 J kg^{-1} K^{-1} (359 mJ cm^{-3} K^{-1}) for $\Delta H = 9$ T.

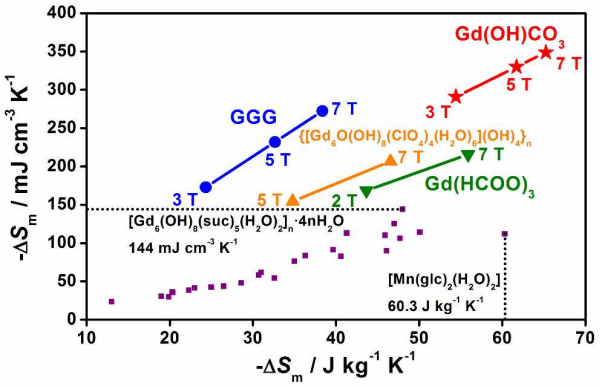

Figure 9 Comparison of the maximum $-\Delta S_m$ with selected ΔH for Gd(OH)CO$_3$(□), Gd(HCOO)$_3$ (▼)[10d], {[Gd$_6$O(OH)$_8$(ClO$_4$)$_4$(H$_2$O)$_6$](OH)$_4$}$_n$ (▲)[9g], GGG (●) and the recently reported molecule-based magnetic refrigerants (■, $\Delta H = 7$ T).

Due to the advantages of high spin density (Gd^{3+} takes up 67% in the formula CHGdO$_4$.) and mass density (5.349 g cm^{-3}), the performance of Gd(OH)CO$_3$ is excellent both in the gravimetric and volumetric units (**Figure 9**). Indeed, it not only surpasses the former record cases with $-\Delta S_{m,\,max}$ of 60.3 kg^{-1} K^{-1} ([Mn(glc)$_2$(H$_2$O)$_2$])[7g] and 144 mJ cm^{-3} K^{-1} ([Gd$_6$(OH)$_8$(suc)$_5$(H$_2$O)$_2$]$_n$·4nH$_2$O),[9h] but also exceeds the recently reported values of {[Gd$_6$O(OH)$_8$(ClO$_4$)$_4$(H$_2$O)$_6$](OH)$_4$}$_n$ ($-\Delta S_{m,\,max}$ = 207 mJ cm^{-3} K^{-1})[9g] and Gd(HCOO)$_3$ ($-\Delta S_{m,\,max}$ = 215.7 mJ cm^{-3} K^{-1}).[10d]

Table 2. Magnetic entropy change for selected molecule-based materials.

Complex[ref]	ΔH (T)	$-\Delta S_{m,\,max}$ (J kg^{-1} K^{-1})	$-\Delta S_{m,\,max}$ (mJ cm^{-3} K^{-1})
***3d*-type**			
{Mn$^{III}_6$Mn$^{II}_4$}[7a-7b]	7	13.0	20.9
{Mn$^{III}_{11}$Mn$^{II}_6$}[7c]	7	13.3	21.8
{Mn$^{III}_6$Mn$^{II}_4$}[7b]	7	17.0	26.2
{Mn$^{II}_4$}[7d]	5	19.3	33.3
{Fe$^{III}_{14}$}[7e]	7	20.3	42.2
{Mn$^{III}_6$Mn$^{II}_8$}[7b]	7	25.0	42.5
[Mn^{II}(Me-ip)(DMF)]$_n$[7f]	8	42.4	66.7
[Mn^{II}(glc)$_2$(H$_2$O)$_2$][7g]	7	60.3	112
***3d*-*4f*-type**			
{Co$^{II}_4$Gd$^{III}_{10}$}[8k]	7	32.6	54.3
{Cu$^{II}_5$Gd$^{III}_4$}[8c]	9	31.0	61.7
{Ni$^{II}_{12}$Gd$^{III}_{36}$}[8e]	7	36.3	83.5
{Co$^{II}_{10}$Gd$^{III}_{42}$}[8h]	7	41.3	113
{[Mn^{II}(H$_2$O)$_6$][Mn^{II}Gd^{III}(oda)$_3$]$_2$·6H$_2$O}$_n$[8j]	7	50.1	114
***4f*-type**			
{[Gd$^{III}_{36}$(NA)$_{36}$(OH)$_{49}$(O)$_6$(NO$_3$)$_6$(N$_3$)$_3$(H$_2$O)$_{20}$]Cl$_2$·28H$_2$O}$_n$[9c]	7	39.7	91.3
{[Gd$^{III}_2$(IDA)$_3$]·2H$_2$O}$_n$[9d]	7	40.6	101
[Gd^{III}(OAc)$_3$(H$_2$O)$_{0.5}$]$_n$[10b]	7	47.7	106
[Gd^{III}(HCOO)(OAc)$_2$(H$_2$O)$_2$]$_n$[10c]	7	45.9	110
[Gd^{III}(C$_4$O$_4$)(OH)(H$_2$O)$_4$]$_n$[9e]	9	47.3	113
{Gd$^{III}_{48}$}[9i]	7	43.6	121
[Gd^{III}(HCOO)(bdc)]$_n$[9b]	9	47.0	125
[Gd$^{III}_6$(OH)$_8$(suc)$_5$(H$_2$O)$_2$]$_n$[9h]	7	48.0	144
{[Gd$^{III}_6$O(OH)$_8$(ClO$_4$)$_4$(H$_2$O)$_6$](OH)$_4$}$_n$[9g]	7	46.6	207
[Gd^{III}(HCOO)$_3$]$_n$[10d]	7	55.9	216
[Gd^{III}(OH)CO$_3$]$_n$ (This work)	3	54.4	291
	5	61.7	330
	7	66.4	355

Me-ip = 5-methylisophthalate, glc = glycolate, oda = oxydiacetate, NA = nicotinate, IDA = iminodiacetate, bdc = benzenedicarboxylate, suc = succinate.

Since the employment of high magnetic field may not be suitable in all circumstances for the technical and economical consideration, the cooling capability under modest fields is of great importance. In this consideration $Gd(OH)CO_3$ is also excellent, e.g. already surpasses commercial GGG whose $-\Delta S_{m,max} \approx 24$ J kg^{-1} K^{-1} (173 mJ cm^{-3} K^{-1}) for $\Delta H = 3$ T.[5] This prominent feature, along with the remarkable ΔS_m and ΔT_{ad} in higher applied field, further highlights the promising cooling power and energy efficiency of $Gd(OH)CO_3$.

DFT calculation

To provide a supporting elucidation to the magnetic interactions between the Gd(III) ions, theoretical calculation using DFT-GGA method with CASTEP code has been performed.[14] We consider four different Gd-O-Gd coupling interactions J_1-J_4 between Gd^{3+} ions in a (*a 2b c*) super-cell (**Figures 10 and S3a**). J_1 is the intra-chain exchange mediated by OH^- both and CO_3^{2-} groups, while J_2-J_4 are inter-chain exchange through CO_3^{2-} only. To determine the values of these exchange parameters, we built five ordered spin states (**Figure S3b-f**) and calculated the energy differences according to the following Hamiltonian:

$$\hat{H} = -\sum_{i<j} J_{ij} S_i S_j$$

where J_{ij} (=J_1, J_2, J_3, J_4) is the magnetic exchange-coupling constants between the spin sites i and j, and S_i and S_j are the spin angular momentum operators at the spin sites i and j, respectively.

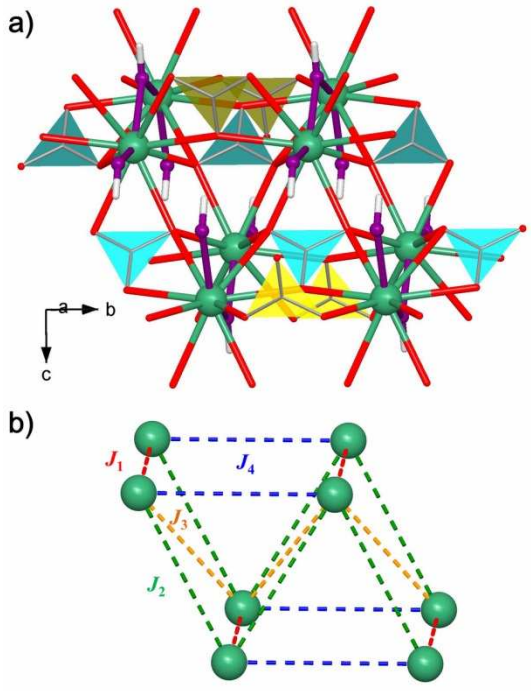

Figure 10 a) A (*a 2b c*) super-cell of $Gd(OH)CO_3$ showing the exchange pathways by OH^- (purple chains) and CO_3^{2-} (blue and yellow triangles). Colour Codes: Gd, green; O, red and purple; C, grey; H, light grey. b) Magnetic coupling interactions J_1-J_4 between Gd^{3+} ions.

Table 3 Geometrical parameters associated with spin exchange ways J_1-J_4 in double unit cell (*a 2b c*) of $Gd(OH)CO_3$ and values of J_1-J_4 calculated from the DFT-GGA method.

Exchange	Distance(Å)	Type of Gd-O-Gd Bridges			J (cm^{-1})
	Gd-O-Gd	μ-OH^-	μ-O (CO_3^{2-})	μ_3-O (CO_3^{2-})	U=0
J_1	3.825	1	0	2	-0.163
J_2	5.128	0	0	1	-0.041
J_3	4.207	0	0	2	0.076
J_4	4.885	0	1	0	-0.073

By applying the energy expressions obtained for spin dimers with N unpaired spins per spin site (in the present case, N = 7), the total spin exchange energies per unit cell of the five spin states are written as:

$$E_{FM} = (-4J_1 - 6J_2 - 3J_3 - 4J_4) * N^2 / 4$$
$$E_{AFM1} = (-4J_1 + 6J_2 + 3J_3 - 4J_4) * N^2 / 4$$
$$E_{AFM2} = (4J_1 - 6J_2 + 3J_3 - 4J_4) * N^2 / 4$$
$$E_{AFM3} = (4J_1 + 6J_2 - 3J_3 - 4J_4) * N^2 / 4$$
$$E_{AFM4} = (-4J_1 - 2J_2 - J_3 + 4J_4) * N^2 / 4$$

By mapping the relative energies of the five ordered spin states determined from GGA calculations, we obtained the values (in cm^{-1}) of J_1, J_2, J_3, and J_4 are −0.163, −0.041, 0.076 and −0.073, respectively (**Table 3**). To check whether these values are reasonable, we compared the Weiss constant θ calculated from the obtained J values and the experimental fitting. According to the mean field theory[14] θ and J are related as:

$$\theta = \frac{s(s+1)}{3k_B} \sum_i z_i J_i$$

where the summation runs over all nearest neighbours of a given spin site, and z_i is the number of nearest neighbours connected by the spin exchange parameter J_i. Thus, θ can be approximated as:

$$\theta \approx \frac{63(2J_1 + 2J_2 + 2J_3 + 2J_4)}{12k_B}$$

The obtained θ value is −3.0 K, which fits well with our experimental result of −1.05 K because the GGA calculations usually overestimate the spin exchange interaction.[17a] From the above calculations, we can see that all the spin interactions are very weak due to the internal nature of 4f electrons, which were also observed in other gadolinium compounds.[17b-c] The negative value of J_1 accounts for the strongest antiferromagnetic interaction along the Gd^{3+}-OH^- chains, which dominate the magnetic states of $Gd(OH)CO_3$. However, the positive J_3 shows non-negligible inter chain ferromagnetism. Moreover, the antiferromagnetic J_2 and J_4 lead to competing exchange-coupling interactions in the triangular J_2-J_2-J_4 substructure, and thus on the *bc* plane.[17d] Usually, spin-competition may lead to a large number of degenerate spin-states and delay the magnetic ordering, which is beneficiary to enhancing MCE.

Conclusions

In this study, we demonstrate the single-crystal structure and the experimental evaluation of the magnetocaloric effect of a

polymeric coordination material, the orthorhombic $Gd(OH)CO_3$, by magnetization and heat capacity measurements. It is found that no matter in low or high fields the magnetocaloric effect of $Gd(OH)CO_3$ is competitive to the commercial available material GGG, which makes it a promising material for cryogenic magnetic cooling application.

Acknowledgements

This work was supported by the "973 Project" (2012CB821704 and 2014CB845602), project NSFC (Grant no. 91122032, 21371183, 21121061 and 21201137), the NSF of Guangdong (S2013020013002), Program for Changjiang Scholars and Inno-vative Research Team in University of China (IRT1298), project APVV-0132-11 and the "National 1000 Young Talents" program. Part of the thermodynamic studies was performed in MLTL (http://mltl.eu/), which is supported within the program of Czech Research Infrastructures (project no. LM2011025).

Notes and references

[a] *Key Laboratory of Bioinorganic and Synthetic Chemistry of Ministry of Education, State Key Laboratory of Optoelectronic Materials and Technologies, School of Chemistry & Chemical Engineering, Sun Yat-Sen University, Guangzhou, 510275, China. E-mail: tongml@mail.sysu.edu.cn*
[b] *Frontier Institute of Science and Technology, and College and Science, Xi'an Jiaotong University, Xi'an 710054, China. E-mail: chaowu@mail.xjtu.edu.cn; zheng.yanzhen@mail.xjtu.edu.cn*
[c] *Institut für Festkörperforschung, Forschungszentrum Jülich 52425 Jülich, Germany.*
[d] *Centre of Low Temperature Physics Faculty of Science, P.J. Šafárik University and Institute of Experimental Physics SAS, Park Angelinum 9, 041 54 Košice, Slovakia. E-mail: martin.orendac@upjs.sk*
[e] *Faculty of Mathematics and Physics, Department of Condensed Matter Physics, Charles University, Ke Karlovu 5, CZ-12116 Prague 2, Czech Republic.*

† Electronic Supplementary Information (ESI) available: Additional crystallography tables and figures of magnetic properties. See DOI: 10.1039/b000000x/

1 E. Warburg, *Ann. Phys.*, 1881, **249**, 141.
2 P. Debye, *Ann. Phys.*, 1926, **386**, 1154.
3 W. F. Giauque, *J. Am. Chem. Soc.*, 1927, **49**, 1864.
4 V. K. Pecharsky and K. A. Gschneidner Jr., *J. Magn. Magn. Mater.*, 1999, **200**, 44.
5 B. Baudun, R. Lagnier and B. Salce, *J. Magn. Magn. Mater.*, 1982, **27**, 315.
6 V. Franco, J.S.Bl´azquez, B. Ingale and A. Conde, *Annu. Rev. Mater. Res.*, 2012, **42**, 305.
7 (a) M. Manoli, R. D. L. Johnstone, S. Parsons, M. Murrie, M. Affronte, M. Evangelisti and E. K. Brechin, *Angew. Chem Int. Ed.*, 2007, **119**, 4540; (b) M. Manoli, A. Collins, S. Parsons, A. Candini, M. Evangelisti and E. K. Brechin, *J. Am. Chem. Soc.*, 2008, **130**, 11129; (c) S. Nayak, M. Evangelisti, A. K. Powell, J. Reedijk, *Chem. Eur. J.,* 2010, **16**, 12865; (d) J.-P. Zhao, R. Zhao, Q. Yang, B.-W. Hu, F.-C. Liu and X.-H. Bu, *Dalton Trans*., 2013, **42**, 14509; (e) R. Shaw, R. H. Laye, L. F. Jones, D. M. Low, C. Talbot-Eeckelaers, Q. Wei, C. J. Milios, S. Teat, M. Helliwell, J.Raftery, M. Evangelisti, M. Affronte, D. Collison, E.K. Brechin and E. J. L. McInnes, *Inorg. Chem*., 2007, **46**, 4968; (f) C.-B. Tian, R.-P. Chen, C. He, W.-J. Li, Q. Wei, X.-D. Zhang and S.-W. Du, *Chem. Commun.,* 2014, **50**, 1915; (g) Y.-C. Chen, J.-L. Liu, J.-D. Leng, F.-S. Guo, P. Vrábel, M. Orendáč, J. Prokleška, V. Sechovský and M.-L. Tong, *Chem. Eur. J*., 2014, **20**, 3029.
8 (a) G. Karotsis, M. Evangelisti, S. J. Dalgarno and E. K. Brechin, *Angew. Chem. Int. Ed.,* 2009, **48**, 9928; (b) G. Karotsis, S. Kennedy, S. J. Teat, C. M. Beavers, D. A. Fowler, J. J. Morales, M. Evangelisti, S. J. Dalgarno and E. K. Brechin, *J. Am. Chem. Soc.,* 2010, **132**, 12983; (c) S. K. Langley, N. F. Chilton, B. Moubaraki, T. Hooper, E. K. Brechin, M. Evangelisti and K. S. Murray, *Chem. Sci.,* 2011, **2**, 1166; (d) Y.-Z. Zheng, M. Evangelisti and R. E. P. Winpenny, *Angew. Chem. Int. Ed.,* 2011, **50**, 3692; (e) J.-B. Peng, Q.-C. Zhang, X.-J. Kong, Y.-P. Ren, L.-S. Long, R.-B. Huang, L.-S. Zheng and Z. Zheng, *Angew. Chem. Int. Ed.,* 2011, **50**, 10649; (f) T. N. Hooper, J. Schnack, S. Piligkos, M. Evangelisti and E. K. Brechin, *Angew. Chem. Int. Ed.,* 2012, **51**, 4633. (g) Y.-Z. Zheng, M. Evangelisti, F. Tuna and R. E. P. Winpenny, *J. Am. Chem.Soc.,* 2012, **134**, 1057; (h) J.-B. Peng, Q.-C. Zhang, X.-J. Kong, Y.-Z. Zheng, Y.-P. Ren, L.-S. Long, R.-B. Huang, L.-S. Zheng and Z. Zheng, *J. Am. Chem. Soc.,* 2012, **134**, 3314; (i) J.-D. Leng, J.-L. Liu and M.-L. Tong, *Chem. Commun.*, 2012, **48**, 5286; (j) F.-S. Guo, Y.-C. Chen, J.-L. Liu, J.-D. Leng, Z.-S. Meng, P. Vrábel, M. Orendáč and M.-L. Tong, *Chem. Commun.,* 2012, **48**, 12219; (k) E. M. Pineda, F. Tuna, R. G. Pritchard, A. C. Regan, R. E. P. Winpenny and E. J. L. McInnes, *Chem. Commun.,* 2013, **49**, 3522; (l) J.-L. Liu, Y.-C. Chen, Q.-W. Li, S. Gómez-Coca, D. Aravena, E. Ruiz, W.-Q. Lin, J.-D. Leng, M.-L. Tong, *Chem. Commun.*, 2013, **49**, 6549; (m) Z.-M. Zhang, L.-Y. Pan, W.-Q. Lin, J.-D. Leng, F.-S. Guo, Y.-C. Chen, J.-L. Liu, M.-L. Tong, *Chem. Commun.*, 2013, **49**, 8081; (n) J.-L. Liu, Y.-C. Chen, Q.-W. Li, S. Gómez-Coca, D. Aravena, E. Ruiz, J.-D. Leng, M.-L. Tong, *Chem. Eur. J*., 2013, **19**, 17567.
9 (a) R. J. Blagg, F. Tuna, E. J. L. McInnes and R. E. P. Winpenny, *Chem. Commun*. 2011, **47**, 10587; (b) R. Sibille, T. Mazet, B. Malaman, M. François, *Chem. Eur. J*., 2012, **18**, 12970; (c) M. Wu, F. Jiang, X. Kong, D. Yuan, L. Long, S. A. Al-Thabaiti and M. Hong, *Chem. Sci*., 2013, **4**, 3104; (d) J.-M. Jia, S.-J. Liu, Y. Cui, S.-D. Han, T.-L. Hu and X.-H. Bu, *Cryst. Growth Des*., 2013, **13**, 4631; (e) S. Biswas, A. Adhikary, S. Goswami and S. Konar, *Dalton Trans*., 2013, **42**, 13331; (f) L.-X. Chang, G. Xiong, L. Wang, P. Cheng and B. Zhao, *Chem. Commun*., 2013, **49**, 1055; (g) Y.-L. Hou, G. Xiong, P.-F. Shi, R.-R. Cheng, J.-Z. Cui and B. Zhao, *Chem. Commun*., 2013, **49**, 6066; (h) Y.-C. Chen, F.-S. Guo, Y.-Z. Zheng, J.-L. Liu, J.-D. Leng, R. Tarasenko, M. Orendáč, J. Prokleška, V. Sechovský and M.-L. Tong, *Chem. Eur. J*., 2013, **19**, 13504; (i) F.-S. Guo, Y.-C. Chen, L.-L. Mao, W.-Q. Lin, J.-D. Leng, R. Tarasenko, M. Orendáč, J. Prokleška, V. Sechovský and M.-L. Tong, *Chem. Eur. J*., 2013, **19**, 14876.
10 (a) M. Evangelisti, O. Roubeau, E. Palacios, A. Camín, T. N. Hooper, E. K. Brechin and J. J. Alonso, *Angew. Chem. Int. Ed.*, 2011, **50**, 6606; (b) F.-S. Guo, J.-D. Leng, J.-L. Liu, Z.-S. Meng and M.-L. Tong, *Inorg. Chem.*, 2012, **51**, 405; (c) G. Lorusso, M. A. Palacios, G. S. Nichol, E. K. Brechin, O. Roubeau and M. Evangelisti, *Chem. Commun.*, 2012, **48**, 7592; (d) G. Lorusso, J. W. Sharples, E. Palacios, O. Roubeau, E. K. Brechin, R. Sessoli, A. Rossin, F. Tuna, E. J. L. McInnes, D. Collison and M. Evangelisti, *Adv. Mater.*, 2013, **25**, 4653; (e) K. Qian, B. Wang, Z. Wang, G. Su and S. Gao, *Acta Chim. Sin.*, 2013, **71**, 1022.
11 (a) Yu. I. Spichkin, A. K. Zvezdin, S. P. Gubin, A. S. Mischenko and A. M. Tishin, *J. Phys. D*, 2001, **34**, 1162; (b) M. Evangelisti and E. K. Brechin, *Dalton Trans*., 2010, **39**, 4672; (c) R. Sessoli, *Angew. Chem. Int. Ed.*, 2012, **51**, 43; (d) J. W. Sharples and D. Collison, *Polyhedron*., 2013, **54**, 91; (e) Y.-Z. Zheng, G.-J. Zhou, Z. Zheng and R. E. P. Winpenny, *Chem. Soc. Rev*., 2013, **43**, 1462.
12 (a) K. A. Gschneidner Jr. and V. K. Pecharsky, *Annu. Rev. Mater. Sci.,* 2000, **30**, 387; (b) K. A. Gschneidner Jr., V. K. Pecharsky and A. O. Tsokol, *Rep. Prog. Phys.*, 2005, **68**, 1479.
13 (a) G. M. Sheldrick, *Acta Cryst.*, 2008, ***A64***, 112; (b) A. L. Spek, *Acta Cryst*., 2009, **D65**, 148.
14 (a) S. J. Clark, M. D. Segall, C. J. Pickard, P. J. Hasnip, M. J. Probert, K. Refson and M. C. Payne, *Z. Kristallogr*., 2005, **220**, 567; (b) J. P. Perdew, K. Burke and M. Ernzerhof, *Phys. Rev. Lett*., 1996, **77**, 3865; (c) J. D. Pack and M. J. Monkhorst, *J. Phys. Rev. B*, 1977, **16**, 1748; (d) D. Zhang, R. K. Kremer, P. Lemmens, K. Y. Choi, J. Liu, M. H. Whangbo, H. Berger, Y. Skourski and M. Johnsson, *Inorg. Chem.*, 2011, **50**, 12877.
15 (a) T. Tahara, I. Nakai, R, Miyawaki and S. Matsubara, *Z. Kristallogr.*, 2007, **222**, 326; (b) H.-S., Sheu, W.-J., Shih, W.-T. Chuang, I.-F. Li and F.-S Yeh, *J. Chin. Chem. Soc*., 2010, **57**, 938; (c) K. Michiba, T.Tahara, I. Nakai, R. Miyawaki and S. Matsubara, *Z. Kristallogr.*, 2011, **226**, 518.
16 (a) M. Affronte, J. C. Lasjaunias and A. Cornia, *Eur. Phys. J. B*, 2000, **15**, 633; (b) M. Evangelisti, F. Luis, L. J. de Jongh and M. Affronte, *J. Mater. Chem.,* 2006, **16**, 2534.

17 (a) H. J. Koo and M. H. Whangbo, *Inorg. Chem*., 2008, **47**, 4779; (b) S. T. Hatscher and W. Urland, *Angew. Chem. Int. Ed.*, 2003, **42**, 2862; (c) L. E. Roy and T. Hughbanks, *J. Am. Chem. Soc.*, 2006, **128**, 568; (d) J. Richter, J. Schulenberg, A. Honecher, *Quantum Magnetism in Two Dimensions: From Semi-classical Néel Order to Magnetic Disorder* in *Quantum Magnetism* (Eds.: U. Schollwöck, J. Richter, D. J. J. Farnell, R. F. Bishop), Springer, Berlin, 2004.

Graphical TOC

The magnetocaloric effect of orthorhombic $Gd(OH)CO_3$ has been experimentally studied, which exhibits $-\Delta S_m$ up to 66.4 J kg^{-1} K^{-1} (355 mJ cm^{-3} K^{-1}) for ΔH = 7 T and T = 1.8 K.